Simultaneous subchannel data updating for multiple channels of 16-quadrature amplitude modulation signals using a single periodically poled lithium niobate waveguide

Hao Huang,[1,*] Jeng-Yuan Yang,[1] Xiaoxia Wu,[1] Salman Khaleghi,[1] Morteza Ziyadi,[1] Moshe Tur,[2] Carsten Langrock,[3] Martin M. Fejer,[3] Loukas Paraschis,[4] and Alan E. Willner[1]

[1]*Department of Electrical Engineering, University of Southern California, Los Angeles, California 90089, USA*

[2]*School of Electrical Engineering, Tel-Aviv University, Tel-Aviv 69978, Israel*

[3]*Edward L. Ginzton Laboratory, 348 Via Pueblo Mall, Stanford University, Stanford, California 94305, USA*

[4]*Optical Networking, Advanced Technology and Planning, Cisco Systems Inc., San Jose, California 95134, USA*

*Corresponding author: haoh@usc.edu

Subchannel data updating of high-order modulation format signals using cascaded sum- and difference-frequency generation in a single periodically poled lithium niobate waveguide is demonstrated. One quadrature phase-shift-keying subchannel of a 16-quadrature amplitude modulation (QAM) signal at 40 Gbit/s is successfully updated, with an optical signal-to-noise ratio (OSNR) penalty of ~2 dB for return-to-zero and ~4 dB for non-return-to-zero at a bit-error rate (BER) of 2×10^{-3}. Simultaneous processing of four wavelength-multiplexed 16-QAM signals with an average OSNR penalty of 4.5 dB at a BER of 2×10^{-3} is also demonstrated.   © 2012 Optical Society of America
   OCIS codes: 060.2330, 190.4410.

High-order advanced modulation formats have attracted significant interest due to their capability of achieving higher spectral efficiency through data modulation on both amplitude and phase so that each symbol carries more information [1,2]. On the other hand, data grooming with a flexible granularity is potentially desirable in a dynamic and heterogeneous network to meet the demands of variable traffic [3]. Typically, a 16-quadrature amplitude modulation (QAM) signal carries 4 bits of information in each symbol and can be considered as two independent quadrature phase-shift-keying (QPSK) subchannels at the same baud rate. Therefore, a laudable goal would be to process independent subchannels of a 16-QAM signal separately, e.g., data erasing and updating, for data-grooming applications.

The processing of subchannels in a signal with higher-order modulation format has been reported in the literature, including multiplexing of three on–off-keying (OOK) data streams into an 8-PSK signal [4] and two QPSK channels into a star 16-QAM signal using cross-phase modulation [5]. Multiplexing of four OOK signals into a rectangular 16-QAM has been proposed using a nonlinear optical loop mirror [6]. Extracting a DPSK channel from a QPSK signal and a QPSK from 8-PSK signal were also demonstrated using four-wave mixing [7,8]. However, subchannel manipulation of a rectangular QAM signal in the optical domain, to the best of our knowledge, has not been addressed.

In this Letter, we experimentally demonstrate subchannel data erasing/updating for a single channel 16-QAM signal using a periodically poled lithium niobate (PPLN) waveguide [9]. We further show the parallel processing capability by simultaneously updating four wavelength-division-multiplexed (WDM) 16-QAM channels. For a single channel 16-QAM signal at 40 Gbit/s, an optical signal-to-noise ratio (OSNR) penalty of ~2 dB for

return-to-zero (RZ) operation and 4 dB for non-return-to-zero (NRZ) operation is observed at a bit-error rate (BER) of 2×10^{-3} [forward error correction threshold]. For the parallel processing of four WDM NRZ-16-QAM signals, the average OSNR penalty at BER of 2×10^{-3} is ~4.5 dB.

The concept of subchannel data updating is shown in Fig. 1. In general, a data channel with a 16-QAM
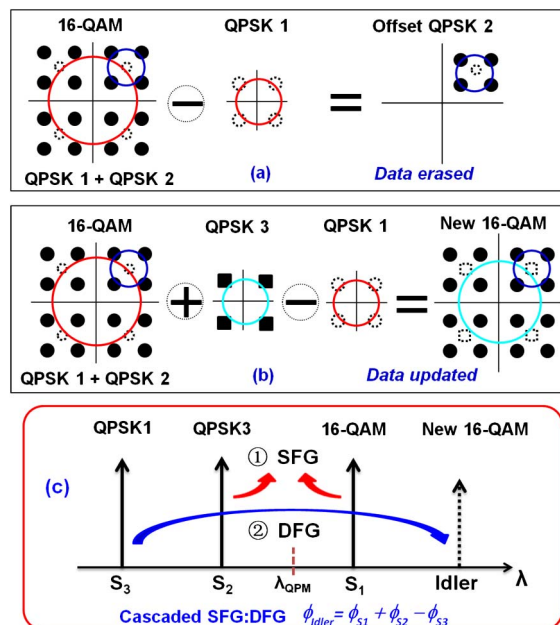

Fig. 1. (Color online) Concept and principle. (a) Concept of data erasing. (b) Concept of data updating. The symbols "plus" and "minus" indicate phase addition and subtraction, respectively. (c) Principle of data updating using cascaded ① SFG and ② DFG in a PPLN waveguide. QPM, quasi-phase matching; SFG/DFG, sum-/difference-frequency generation.

modulation format includes two independent QPSK subchannels. One QPSK (QPSK 1) determines the quadrant of the signal vector in the constellation plane, and the other (QPSK 2) determines the location within each quadrant. Therefore, the data carried by one subchannel can be erased if the phase of QPSK 1 is canceled by phase subtraction between the 16-QAM signal and a synchronized QPSK 1 signal, which potentially could be extracted from the same 16-QAM signal, leaving the other subchannel as an offset QPSK signal, as shown in Fig. 1(a). Furthermore, a new 16-QAM signal can be obtained if a different QPSK signal (QPSK 3) is induced by phase addition between the offset QPSK and the new QPSK, i.e., data updating, as shown in Fig. 1(b). As a result, data on one subchannel is rewritten, while the information on the other subchannel is maintained. Following the concept described above, Fig. 1(c) shows the principle of phase addition/subtraction based on the sum-/difference-frequency generation (SFG/DFG) in a PPLN waveguide [10]. Three signals (S1, S2, and S3, corresponding to 16-QAM, QPSK 3, and QPSK 1, respectively) are fed into the PPLN waveguide. SFG between S1 and S2 happens first, followed by the DFG with S3. In principle, an idler will be generated, following the linear phase relationship expressed as $\Phi_{\mathrm{idler}} = \Phi_{S1} + \Phi_{S2} - \Phi_{S3}$. Specifically, if S2 is a continuous wave (CW) with a constant phase, and S3 is a QPSK signal that carries the same information as the subchannel QPSK 1, the phase of the generated idler would be $\Phi_{S1} - \Phi_{S3}$. As a result, this subchannel will be erased with the other subchannel (QPSK2) remaining as an offset QPSK. Accordingly, if S2 carries a new QPSK signal (QPSK 3), its phase will be added into the offset QPSK (QPSK 2) and a new 16-QAM signal with one subchannel being updated can be obtained. It is noted that the updated signal is carried on a different wavelength after processing; therefore the changing of the filter at the receiver might be required, or an additional wavelength conversion stage could be used to convert it back to the original wavelength.

The experimental setup is illustrated in Fig. 2. The 16-QAM is generated through a serial modulation method, in which two IQ modulators driven by four independent 10 Gbit/s binary data channels modulate a CW laser
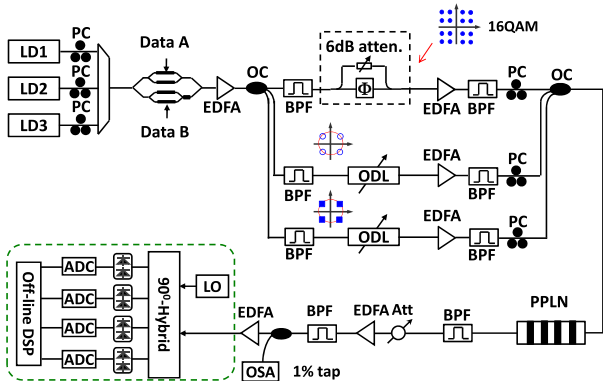
Fig. 2.   (Color online) Experimental setup. LD, laser diode; PC, polarization controller; EDFA, erbium-doped fiber amplifier; OC, optical coupler; BPF, band-pass filter; ODL, optical delay line; OSA, optical spectral analyzer; LO, local oscillator; ADC, analog-to-digital converter; DSP, digital signal processing.
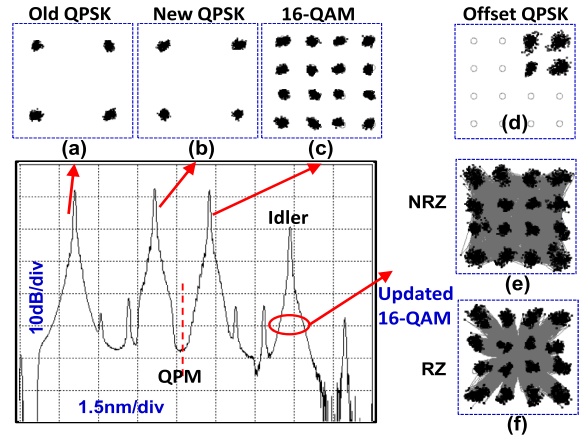
Fig. 3.   (Color online) Optical spectrum and constellations. (a)–(c) Back-to-back QPSK signals and NRZ 16-QAM signal. (d) Offset QPSK with the other subchannel erased. (e) Updated NRZ 16-QAM. (f) Updated RZ 16-QAM.

(LD1). The first IQ modulator generates a typical QPSK channel (QPSK 1), and the second IQ modulator generates an offset QPSK channel (QPSK 2). In this proof-of-concept experiment, the second IQ modulator is replaced with a unbalanced delay-line interferometer, which is able to generate a 16-QAM signal by vector addition between two QPSK signals, with one of them attenuated by 6 dB. Two other CW lasers (LD2 and LD3) are also coupled into the first IQ modulator, and then properly delayed to emulate the known QPSK 1 channel and the unknown QPSK 3 channel, respectively. Three tunable delay lines are used to synchronize three signals in the time domain. After amplification to ~15 dBm, all three channels are coupled into a PPLN waveguide with a length of ~4 cm. The idler is filtered out from the output signals and sent to a coherent receiver for BER measurement. The spectrum at the output of the PPLN waveguide is shown in Fig. 3. An idler with a conversion efficiency of approximately −12 dB is obtained. Figures 3(a)–3(c) display the measured constellations of the QPSK 1 and new QPSK 3, as well as the 16-QAM signal before coupling into the PPLN waveguide. First, we verify the information-erasing process using a CW instead of a new QPSK signal for S2. After SFG/DFG, an offset QPSK signal is obtained as the idler, as shown in Fig. 3(d). One of the subchannels (the old QPSK, i.e., QPSK 1) of the 16-QAM signals has been successfully erased. We further change S2 into a QPSK signal (the new QPSK, i.e., QPSK 3). A new NRZ 16-QAM signal with one QPSK subchannel being updated is
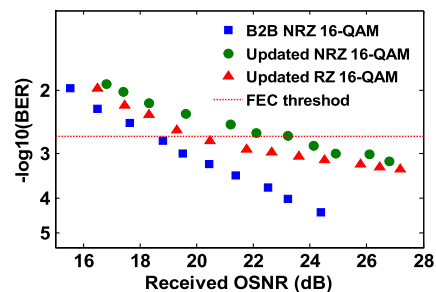
Fig. 4.   (Color online) BER performance as a function of the received OSNR.
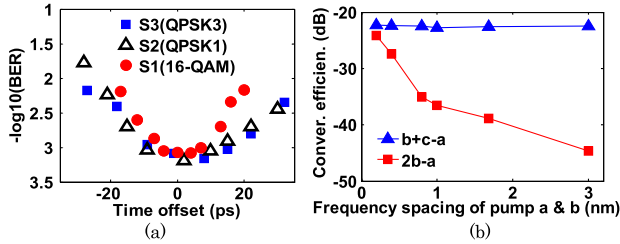
Fig. 5.   (Color online) (a) BER versus relative time offset among three input signals (OSNR = 20 dB). (b) Conversion efficiencies as functions of frequency spacing between pump a and pump b. ($\lambda_c - \lambda_b = 1.6$ nm)
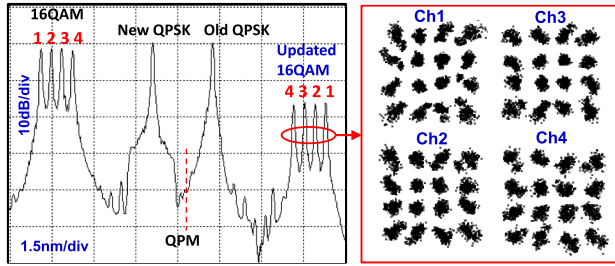

Fig. 6.   (Color online) Optical spectral of WDM NRZ 16-QAM information updating and the constellations for each updated channel.

Fig. 7.   (Color online) BER performance as a function of the received OSNR for each WDM channel.

obtained, as shown in Fig. 3(e). We also demonstrate simultaneous information updating and format conversion into a RZ 16-QAM signal by pulse carving $S3$ through a Mach–Zehnder modulator, as shown in Fig. 3(f). Figure 4 shows the measured BER curves of the back-to-back and updated 16-QAM signals in both RZ and NRZ formats at 10 Gbaud/s. The observed power penalty at a BER of 2×10^{-3} is ~2 dB for RZ 16-QAM and ~4 dB for NRZ 16-QAM. RZ format performs better than NRZ due to that RZ has a higher peak power and consequently a higher conversion efficiency than NRZ with the same average power. Figure 5(a) shows the BER performance as a function of the relative time offset among three input signals with an OSNR of 20 dB. The time offset tolerance to achieve BER of $<2 \times 10^{-3}$ is ~20 ps for two QPSK signals and ~15 ps for a NRZ 16-QAM signal. It can be seen from the optical spectrum that besides the desired idler (i.e., $\lambda_b + \lambda_c - \lambda_a$), there are also some other idlers with a lower efficiency from unwanted interaction. The efficiency of both the desired and undesired idlers (e.g, $2\lambda_b - \lambda_a$) as functions of the frequency spacing between pump a and b (see Fig. 3) are plotted in Fig. 5(b) ($\lambda_c - \lambda_b$ is fixed at 1.6 nm). The undesired interaction efficiency increase dramatically when the frequency of pump a approaches pump b, since their phase-matching condition is more closely satisfied.

To show the capability of parallel processing, we demonstrate simultaneously processing of four-channel WDM 16-QAM signals in a single stage, provided that these four 16-QAM signals share the same data on one of their subchannels. The shared subchannel (QPSK1) could be erased and subsequently updated by phase
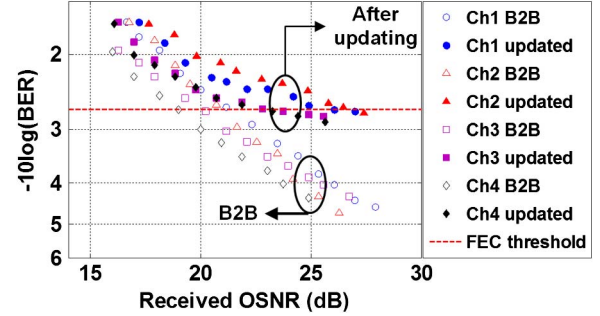
subtraction/addition. The observed optical spectrum is shown in Fig. 6. Two amplified QPSK signals (QPSK1 and QPSK3) at 1548.09 and 1550.14 nm with a power of ~18.2 dBm, together with four NRZ 16-QAM signals with 50 GHz wavelength spacing (1544.74, 1545.14, 1545.54, and 1545.94 nm), all around 15.4 dBm, are coupled into the PPLN waveguide. As expected, four idlers are generated, corresponding to four updated NRZ 16-QAM signals; the constellations of each signal are shown in Fig. 6. The BER of each channel is also measured and plotted in Fig. 7. Due in part to the crosstalk between adjacent channels, the WDM signal processing performance is not as good as a single channel, but all four channels can still achieve a BER below 2×10^{-3}. An average OSNR penalty of ~4.5 dB at a BER of 2×10^{-3} is observed for the data erasing/updating operations.

References

1. A. H. Gnauck, P. J. Winzer, S. Chandrasekhar, X. Liu, B. Zhu, and D. W. Peckham, J. Lightwave Technol. **29**, 373 (2011).
2. T. Omiya, K. Toyoda, M. Yoshida, and M. Nakazawa, in *Optical Fiber Communication Conference*, OSA Technical Digest (Optical Society of America, 2012), paper OM2A.7.
3. N. Kataoka, N. Wada, K. Sone, Y. Aoki, H. Miyata, H. Onaka, and K. Kitayama, J. Lightwave Technol. **24**, 88 (2006).
4. K. Mishina, S. Kitagawa, and A. Maruta, Opt. Express **15**, 8444 (2007).
5. X. Wu, J. Wang, H. Huang, and A. E. Willner, in *CLEO: 2011—Laser Applications to Photonic Applications*, OSA Technical Digest (CD) (Optical Society of America, 2011), paper CThH4.
6. G. Huang, Y. Miyoshi, A. Maruta, Y. Yoshida, and K.-I. Kitayama, J. Lightwave Technol. **30**, 1342 (2012).
7. G.-W. Lu and T. Miyazaki, Opt. Express **17**, 13346 (2009).
8. G.-W. Lu, E. Tipsuwannakul, T. Miyazaki, C. Lundström, M. Karlsson, and P. A. Andrekson, J. Lightwave Technol. **29**, 2460 (2011).
9. H. Huang, J.-Y. Yang, X. Wu, S. Khaleghi, M. Tur, C. Langrock, M. Fejer, and A. Willner, in *CLEO: 2012 Laser Applications to Photonic Applications*, OSA Technical Digest (CD) (Optical Society of America, 2012), paper CM2B.3.
10. H. Tan, G. P. Banfi, and A. Tomaselli, Appl. Phys. Lett. **63**, 2472 (1993).